A kinematic coupling mechanism with binary electromagnetic actuators for high-precision positioning

Matteo Russo, *Member, IEEE*, Jorge Barrientos-Diez, *Member, IEEE*, and Dragos Axinte

***Abstract*—Rather than working in a continuous range of motion, binary actuators can only maintain two positions. This lack of flexibility is compensated by high accuracy, repeatability, and reliability. These features make binary-actuated mechanisms appealing for space exploration systems, repetitive pick & place tasks, and biomedical applications. This paper introduces a novel class of binary-actuated mechanisms driven by electromagnets. As these systems rely on the extreme positions of their binary actuators for positioning, the proposed design aims to increase repeatability with a kinematic coupling. By inverting the polarity of its electromagnets, the configuration of the mechanism can be changed from a discrete state to another one. Thus, when the actuation is known, the pose of the system can be accurately computed without any external feedback. A sensorless design simplifies both the control and the architecture of the proposed design, as well as reducing manufacturing and maintenance costs. The conceptual design of the proposed class of mechanisms is described through two examples with three and four configurations, and alternative designs with higher mobility are discussed. Then, a kinematic synthesis procedure is discussed. Finally, the advantages of asymmetric and irregular designs are outlined. Overall, the proposed mechanisms are suited to a wide range of applications that require a rapid, accurate and interchangeable positioning of sensors and tools.**

***Index Terms*—Manipulators, Kinematics, Robot control, Binary actuators, Modular robots**

I. Introduction

WHEREAS conventional actuators are continuous systems that can achieve any positioning within their motion range, binary actuators can only maintain one of two possible states at their extreme positions [1]. Thus, the behavior of a binary actuator can be controlled with an on/off—or open/close—switch that triggers a discrete change in state. Some examples of binary actuators are pneumatic cylinders, artificial muscles, elastic bistable joints, shape-memory alloys (SMA) and dielectric elastomer actuators (DEA) [1-10].

The finite number of states that can be maintained by a binary actuator enables sensorless control [2-6]. In such case, low-level control is significantly simplified and the associated sensors, wiring and electronics can be safely removed without impacting negatively on the system's performance [7-8]. Thus, a system with binary actuation is usually simpler, more robust, and cheaper than an equivalent continuous system. The reduced motion range of binary mechatronic systems can be also compensated by redundant and hyper-redundant architectures, since the performance of a continuous system can be approached as the number of binary actuators increases [3-4].

However, the design of binary mechatronic systems poses several challenges, such as keeping the system lightweight and compact, and complex path planning algorithms for hyper-redundant manipulators, since the number of possible configurations of binary systems grows exponentially with the number of actuators. For example, a binary mechatronic system with 10 actuators has 2^{10} (1024) distinct states. Doubling the motors leads to 2^{20} combinations (approximately 10^6) and doubling again increases the number of distinct states over 10^{12}. Thus, while inverse kinematics can be solved with a brute force search for few actuators, complex approaches are needed for systems with more degrees of freedom, as outlined in [4-6].

Thanks to their unique features, binary-actuated systems are suitable for deployment tasks that require a rapid and/or accurate positioning of sensors and tools, with applications that range from space exploration to surgical robotics. These fields require simple, robust, and reliable mechanisms, and binary devices have often been proposed to meet this need [7-24].

In this paper, a new mechanism concept with binary electromagnetic actuation is proposed for applications that require high-precision positioning, such as reconfigurable fixturing systems for machining [25-26]. By selecting an appropriate kinematic coupling, the proposed design can achieve accurate positioning without sensors for feedback. The electromagnets that actuate the system double up as clutches to maintain the mechanism in its stable states, and the reduced surface contact ensures an efficient motion with negligible friction in the transition from one state to another. The performance of this system is limited by the number of stable configurations, but modular designs can achieve higher degrees of freedom by connecting multiple modules in series or parallel, resulting in a robust, low-cost, high-precision positioning device for tool and sensor deployment.

When compared to previous designs (e.g. [9,18]), the

Submitted for review on XX/XX/2020.

Corresponding author: Matteo Russo (matteo.russo@nottingham.ac.uk)

This work was supported in part by UK EPSRC project Robotics and Artificial Intelligence in Nuclear (RAIN) under grant EP/R026084/1.

M. Russo, J. Barrientos-Diez, and D. Axinte are with the Rolls-Royce UTC in Manufacturing and On-Wing Technology, Faculty of Engineering, University of Nottingham, Nottingham NG8 1BB, United Kingdom (e-mail: {matteo.russo; jorge.barrientosdiez; dragos.axinte}@nottingham.ac.uk).

proposed design is characterized by a higher accuracy and repeatability, as its configurations are defined by a kinematic coupling rather than standard manufacturing or assembly tolerances. Furthermore, this feature removes the need for external sensors, as the pose of the mechanism can be reliably achieved as high-accuracy locators are employed. Finally, the transition between states is triggered by a switch in actuator polarity and characterized by a quick low-friction sliding motion, whereas other bistable actuators like shape-memory alloys have long activation and relaxation times [16].

The aim of this paper is to introduce this novel class of mechanisms with binary electromagnetic actuation, with a focus on their kinematic parameters, control logic, and a design procedure to obtain the geometrical parameters that are required to reach an arbitrary number of given poses, for applications such as industrial pick&place tasks and reconfigurable fixturing systems. In Section II, previous works on the topic are analyzed to explain the design choices of the proposed concept, which is discussed in Section III with details on the actuation, kinematic couplings, and alternative designs. In Section IV, the proposed system is modelled, and a procedure for its kinematic synthesis from prescribed desired frames is presented with two examples. Most of the binary systems in literature are based on regular and symmetric designs. However, irregular and/or asymmetric designs often perform better on prescribed tasks. Therefore, these options are explored in Section V, with a performance comparison with regular symmetric designs.

II. Previous Work

Two bodies of literature are reviewed in this section. First, a brief history of binary-actuated systems is presented, focusing on actuation technologies and applications to identify optimal design choices. Then, kinematic couplings are discussed.

A. Binary mechatronic systems

After three decades of research on the topic, binary mechatronic systems are still an ongoing research field, with a strong theoretical background but very few successful designs. In Table I, the state of the art in binary-actuated devices is summarized by non-exhaustive, representative sampling of publications on the topic. For each publication, the application field and the mean of actuation has been listed.

The analysis of binary-actuated manipulators is based on the seminal work of Chirikjian's research group at Johns Hopkins University in the 1990s [1-3]. By proposing and comparing different approaches to trajectory planning [4] and kinematics [5-6], their early publications provide a theoretical framework for both the synthesis [2] and analysis [3] of these systems.

Other research groups expanded this framework with research on the optimal design of binary manipulators [7-8], but most of the subsequent work on the topic was experimental: in the 2000s, several research groups developed Chirikjian's ideas into functional prototypes. For example, Dubowsky's group at Massachusetts Institute of Technology explored different means of actuation for a binary mechanism based on a module with a three-limbed parallel architecture [9-13]. After comparing the performance of DEAs [9-11], electromagnetic actuators [12], and SMAs [13], they settled on DEAs as optimal mean of actuation for their design, developed for camera and tool positioning in space and biomedical applications.

Whereas DEA solutions were successful for positioning tasks, SMA [14-16] and pneumatics [17] proved to be better for manipulation tasks. Other technologies, such as bistable compliant mechanisms, were also proposed for specific application, such as the monolithic design in [18]. Overall, research trends have shown that DEAs and electromagnetic actuators are favoured in tasks that require accurate positioning but struggle with high payloads [19-24]. Conversely, pneumatics and SMAs are able to withstand higher forces, but at the cost of lower accuracy and efficiency, and increased size.

Since the proposed concept focuses on positioning, the choice of an actuator can be safely narrowed down to DEAs and electromagnets. The latter were chosen because of both technical and practical advantages: electromagnets can double up as clutches to maintain the system in its state against external disturbance; they are also generally cheaper and more accessible, and result in a more robust design overall.

TABLE I
Related Work—Binary Mechatronic Systems

Reference	Actuation	Application
[1-6]	Any	Manipulation
[7]	Any	Manipulation
[8]	Any	Manipulation
[9-11]	DEA[a]	Biomedical
[12]	Electromagnets	Biomedical
[13]	SMA[b]	Space
[14-15]	SMA[b]	Grasping
[16]	SMA	Manipulation
[17]	Pneumatics	Manipulation
[18]	Compliance	Space
[19]	Electromagnets	Tooling
[20-21]	Electromagnets	Flytrap
[22-23]	Electromagnets	Manipulation
[24]	Electromagnets	Origami robots

[a]DEA: Dielectric Elastomer Actuation
[b]SMA: Shape Memory Alloy

B. Kinematic coupling

Binary mechatronic systems often use mechanical stops to provide a repeatable connection between two bodies, relying on large areas in contact at the extreme positions of the actuators to maintain a stable state. Whilst this solution can be fairly accurate, there is a margin of uncertainty given by the redundancy and tolerances of these contacts that can be reduced with a kinematic coupling [27]. A kinematic coupling is a simple mechanical solution that provides a rigid repeatable connection between two objects through six local contact areas [28]. They usually serve applications that require the separation and the repeatable engagement of two objects. Most kinematic couplings are adaptations of one of the two classical configurations, which are the Three-Groove and Kelvin Clamp couplings [27-32]. The main advantage of these solutions lies in their low-cost, simple design that can provide an extremely high repeatability (in the range of 10 μm, as shown in [29-31]).

Given the similar performance of the Three-Groove and Kelvin Clamp couplings, the first [32] has been selected for the mechanisms in Section III because of its symmetrical layout.

However, the constructive solutions shown in this paper are only two examples of implementation of the proposed concept, which can be realized with a wide variety of geometries.

III. Conceptual Design of a Novel Binary System

In its most general form, the device presented in this paper is a modular mechanism that consists of two or more platforms connected by kinematic couplings. In each pair of coupled platforms, the base platform includes the grooves ("pins") of a kinematic coupling for positioning the top platform with pins or spherical features ("balls").

The kinematic coupling plays a double role in the proposed design: it ensures a repeatable positioning of the two platforms in each state, and it guides the transition between distinct states. In each state, the top platform shares at least six local contact points with the base, with each ball touching two of the pins. During the transition from one state to another, the electromagnetic force of the binary actuators forces a rotation of the top platform on a virtual hinge created by sliding surface couplings of two balls on four of the supporting pins. The transition from one state to another is triggered by changes in polarity of the electromagnets in the base, that control the configuration of the system by attracting (+) and repelling (-) the permanent magnets embedded in the top platform.

Two distinct platform design examples are here introduced. The first one, presented in Section III-A, is the simplest module design for the proposed concept, with 2D mobility only, whereas the second one, illustrated in Section III-B, is capable of 3D motion. Moreover, alternative designs are discussed in Section III-C to obtain higher mobility, with solutions that range from stacking modules to increase the degrees of freedom of the system to redundant kinematic couplings to increase the number of states that can be achieved by a single module.

A. *Module design for planar mobility*

A planar example of the proposed concept limited to a 2D motion with three states can be obtained with a cylinder-to-vee kinematic coupling, characterized by an ideally linear contact rather than punctiform contact. This design cannot constrain motion along the normal to the plane of motion, and additional constraints are needed to balance any load in that direction. The states of a 2D concept with the corresponding actuation are illustrated in Fig. 1 and Table II.

The design in Fig. 1 is in a neutral state when the two platforms are connected by the kinematic coupling 0, with the top platform lying parallel to the central surface on the base. The other two states result in the top platform "leaning" to one side. State A is obtained through a rotation of the top platform around the axis defined by the contacts in A1 by attracting magnet A and repelling B. Similarly, state B is obtained through a rotation of the top platform around the axis defined by the contacts in B1 by attracting magnet B and repelling A.

The proposed concept has been validated on a rapid prototyped system, shown in Fig. 2, which has been built with the components listed in Table III. Each module is made of a 3D printed shell, 3 electromagnets, and 3 permanent magnets, with a total weight of 125 g and 90 x 23 x 23 mm in size. The bending angle of the non-neutral states is 8 deg. The permanent magnets can be installed arbitrarily, as the polarity of the electromagnets can be changed accordingly. The prototype is controlled by a commercial microcontroller and motor driver with the logic in Table II, by using the optimal configurations of choice for each state, which can be selected between maximum clutching force and power saving. During the experiments, the prototype has successfully achieved all the possible configurations, and no interference or decrease in performance has been observed because of the proximity of permanent magnets and electromagnets on the same module. The clutching capability of the magnets has also been tested, and the prototype can withstand a load of 20 N in every stable state with the configuration for optimal clutching force.

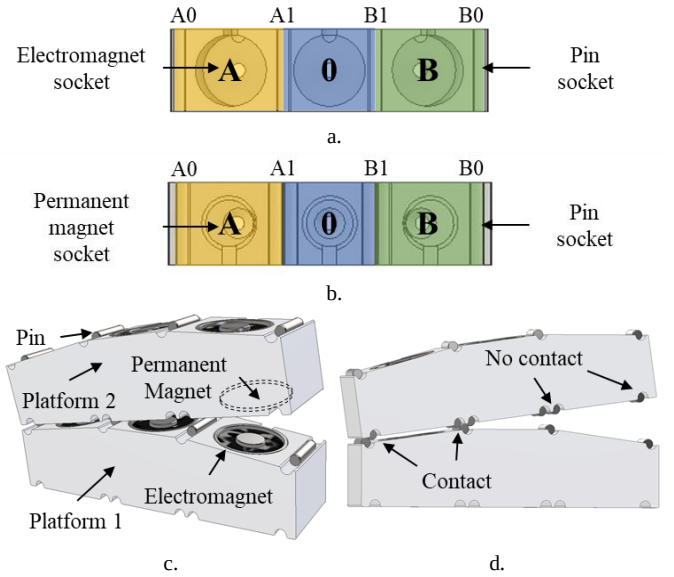

Fig. 1. A modular 2D concept: a. Top view of the base with the electromagnets, with the contacts of the three possible states (0, A, and B) highlighted; b. Bottom view of the top platform with the permanent magnets. c. View of an assembly with main constitutive elements; d. Side view with 2D adaptation of the Three-Groove kinematic coupling.

TABLE II
System States and Corresponding Actuation of 2D Concept

System state	Axis of rotation	Kinematic coupling	0[a]	A[a]	B[a]	Configuration
0[b]	-	A1-B1	+	+	+	
0[c]	-	A1-B1	+	-	-	
0[d]	-	A1-B1	+	=	=	
A[b]	A1	A1-A0	+	+	-	
A[c]	A1	A1-A0	-	+	-	
A[d]	A1	A1-A0	=	+	-	
B[b]	B1	B1-B0	+	-	+	
B[c]	B1	B1-B0	-	-	+	
B[d]	B1	B1-B0	=	-	+	

[a]The state of each binary actuator is (+) when the electromagnet is attracting the corresponding permanent magnet, and (-) when the electromagnet is repelling the corresponding permanent magnet. A state of (=) indicates that the clutch is turned off, neither attracting nor repelling.

[b]Optimal configuration to achieve the desired state with the maximum clutching force.

[c]Suboptimal configuration to achieve the desired state, usually characterized by a lower clutching force than the optimal configuration but with the same power consumption, as all the electromagnets are still on.

[d]Optimal configuration to achieve the desired state with the lowest power consumption.

TABLE III
PROTOTYPE COMPONENTS

Name	Component	Datasheet
Base	3D Printed (ABS Plastic)	-
Top Platform	3D Printed (ABS Plastic)	-
Plate	Laser-cut	-
Controller	Arduino Mega 2560 Rev3	[33]
Motor Driver	Adafruit Motorshield v2	[34]
Electromagnets	Adafruit 5V Electromagnet P20/15	[35]
Permanent Magnets	Eclipse Neodymium Magnet	[36]
Mechanical Elements	Screws, Nuts	-
Coupling Elements	Ball bearings, Dowel pins	-
Electrical Elements	Commercial cables	-

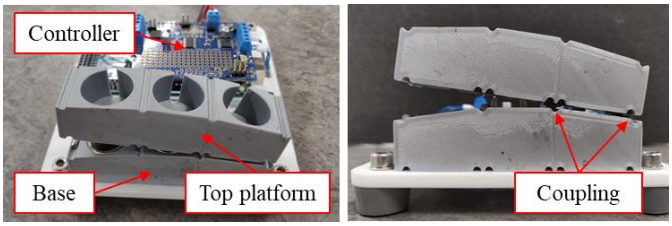

a. b.

Fig. 2. A prototype of the planar design assembled with 3D-printed and laser-cut components, and with commercial electronics: a. Module prototype in with Arduino microcontroller; b. Side view.

B. *Module design for spatial mobility*

A design solution capable of 3D motion can be obtained by connecting two platforms with a Three-Groove kinematic coupling. In each state, the top platform shares exactly six local contacts with the base, with each ball touching two of the pins. The example in Fig. 3 can achieve four different states, which are illustrated in Fig. 4. When the two platforms are connected through the kinematic coupling 0, the system is in a "neutral" state, with the top platform lying parallel to the central surface on the base. This state can be achieved with two distinct symmetrical actuation patterns, with electromagnet 0 attracting permanent magnet 0 and all the other electromagnets either attracting or repelling the respective permanent magnets. The first is preferred for the higher clutching force provided, which allows the system to react to external disturbance better.

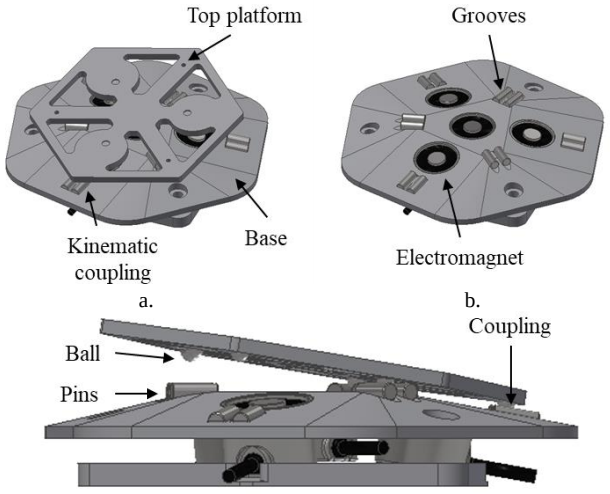

a. b. c.

Fig. 3. Model of the proposed concept: a. Isometric view of a module in a non-neutral state; b. Mechanism base; c. Module side view in a non-neutral state.

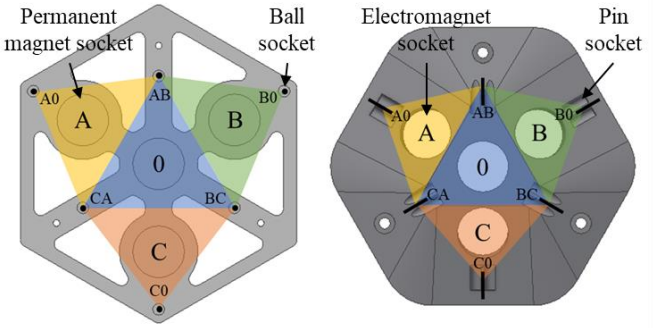

a. b.

Fig. 4. Elements of the proposed concept, with the contacts of the four possible states (0, A, B, and C) highlighted: a. Bottom view of the top platform with the positions of the permanent magnets and the ball sockets; b. Top view of the base with the position of the electromagnets and the pins.

TABLE IV
SYSTEM STATES AND CORRESPONDING ACTUATION OF 3D CONCEPT

System state	Axis of rotation	Kinematic coupling	0[a]	A[a]	B[a]	C[a]	Configuration
0[b]	-	AB-BC-CA	+	+	+	+	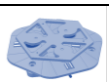
0[c]	-	AB-BC-CA	+	-	-	-	
0[d]	-	AB-BC-CA	+	=	=	=	
A[b]	AB-CA	AB-CA-A0	+	+	-	-	
A[c]	AB-CA	AB-CA-A0	-	+	-	-	
A[d]	AB-CA	AB-CA-A0	=	+	-	-	
B[b]	AB-BC	AB-BC-B0	+	-	+	-	
B[c]	AB-BC	AB-BC-B0	-	-	+	-	
B[d]	AB-BC	AB-BC-B0	=	-	+	-	
C[b]	BC-CA	BC-CA-C0	+	-	-	+	
C[c]	BC-CA	BC-CA-C0	-	-	-	+	
C[d]	BC-CA	BC-CA-C0	=	-	-	+	

[a]The state of each binary actuator is (+) for attraction and (-) for repulsion., whereas (=) indicates a clutch that is turned off.
[b]Optimal configuration to achieve the desired state (max clutching force).
[c]Suboptimal configuration to achieve the desired state.
[d]Optimal configuration to achieve the desired state (low consumption).

The other three states result in the top platform "leaning" on one side. State A is obtained through a rotation of the top platform around the axis defined by contacts AB and CA, by attracting magnet A and repelling B and C. Similarly, state B is obtained through a rotation of the top platform around the axis defined by contacts AB and BC, by attracting magnet B and repelling C and A. Finally, state C is obtained through a rotation around the axis defined by contacts BC and CA, by attracting magnet C and repelling A and B. These system configurations and their actuation are summarized in Table IV.

The proposed concept has also been validated on a rapid prototyped system, with components in Table III and shown in Fig. 5. Each module is made of a 3D printed shell, 4 electromagnets, and 4 permanent magnets, with a total weight of 175 g and 110 x 110 x 22 mm in size. The bending angle of the non-neutral states is 10 deg. The prototype has been controlled with the logic in Table IV, by using the optimal configurations for each state, in order to achieve all the possible configurations. The clutching capability of the magnets has been tested as well, and the prototype can withstand a load of 15 N in every stable state, less than the 2D prototype because of increased platform weight and different geometry.

The transition from the neutral state to any other state has

been measured with a VICON motion capture system with four Vantage 16 cameras (30 Hz, calibration accuracy 0.05 mm), with the results of 8 trials shown in Fig. 6. The motion has always been performed smoothly in less than 0.1 s and with a maximum error of 0.25 deg on the target 10 deg bend, with the top platform rotating around the desired virtual hinge and moving from the central kinematic coupling to the desired one. A slight overshooting (less than 15%) has been observed in 25% of the trials before settling to the desired bending value. The positioning accuracy of the prototype is 0.05 mm, within the manufacturing tolerances on the prototype (0.20 mm for the 3D printed assembly, corresponding approximately to a 0.5 deg tolerance on the bending angle). Furthermore, the reliability of the prototype is proved by an acquired repeatability of 0.07 mm. The peak power consumption during operation is 5.0 W.

However, a direct transition from a non-neutral state to another non-neutral state is not possible. When the actuation switches from one of those configurations to another, the top platform briefly transitions through the neutral state before achieving the target state (see attached video). Even if this behavior has no consequences on the final state of the system, the required transition through the neutral state can be relevant in case of trajectory planning of one or multiple stacked modules of the proposed binary mechatronic system.

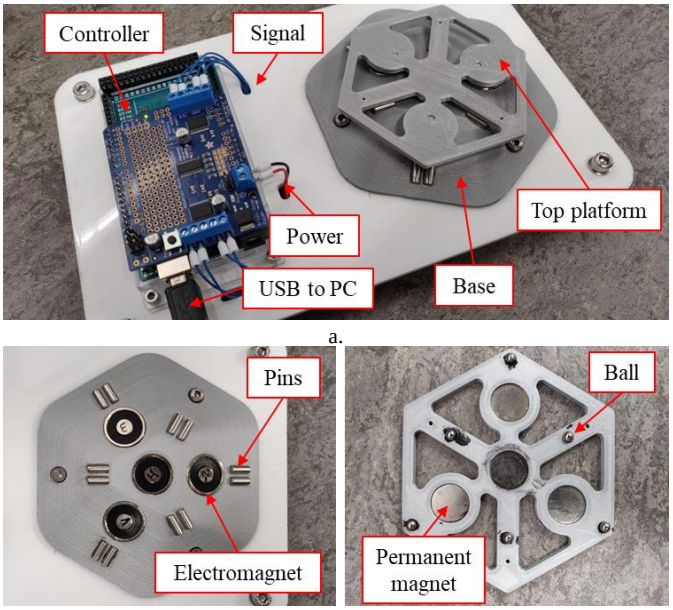

Fig. 5. A prototype of the spatial design: a. Module prototype in neutral state with Arduino microcontroller; b. Bottom view of the top platform; c. Top view of the prototype base.

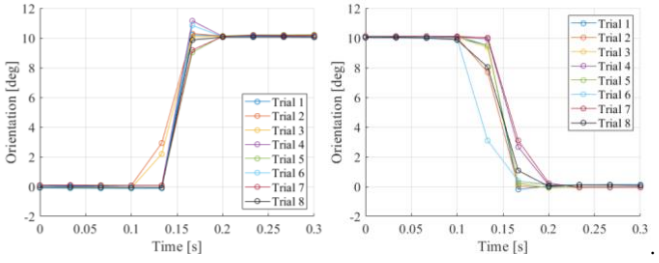

Fig. 6. Acquired angular motion of the platform acquired with a motion capture system: a. Transition from neutral state; b. Transition to neutral state.

C. *Alternative designs for increased mobility*

The number of states and degrees of freedom of the system can be increased by stacking platforms, with the top platform of a module functioning as the base of the following one.

In the example in Fig. 7, based on the design in Section III-A, the permanent magnets and the electromagnets of each module are stacked. Thus, platform i acts as top platform for $i - 1$ and as base for $i + 1$. The number of states of the system is given by all the possible combinations between the states of the single modules. As each module can achieve three states {0, A, B}, and the combined system has nine states {00, 0A, 0B, A0, AA, AB, B0, BA, BB}. The modular 2D concept has been validated on a prototype, which has been successfully tested in all the configurations. Another prototype, in Fig. 8, shows a 3D version of the concept based on the design of Section III-B.

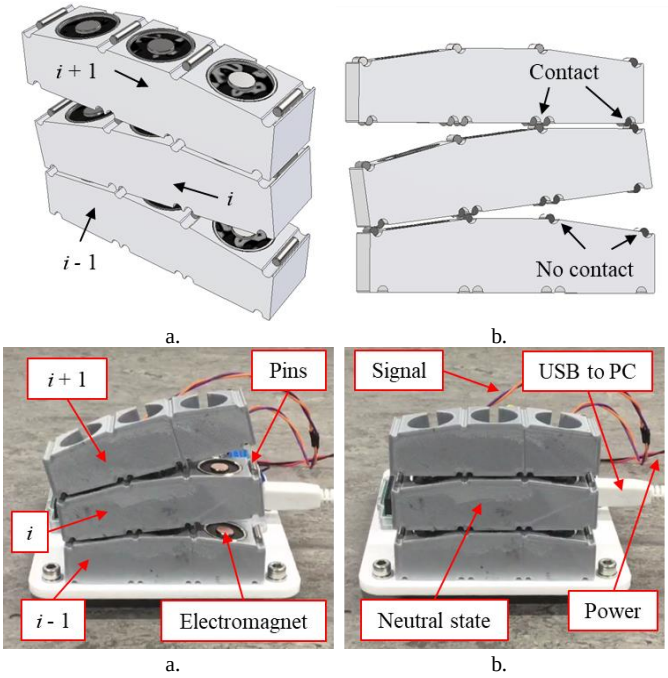

Fig. 7. A modular 2D concept with increased mobility: a. View of an assembly with two stacked modules in non-neutral states; b. Side view with 2D adaptation of the Three-Groove kinematic coupling; c. A prototype with both modules in a non-neutral state; d. A prototype with both modules in a neutral state.

In general, the number of distinct states achievable by such a combined system is equal to n^m, where m is the number of modules and n is the number of states of each module. Thus, by stacking modules, the mobility is increased exponentially. However, as the bottom platform must withstand not only the wrench acting on the system but also the weight of the other platforms, the number of stacked modules is limited by the electromagnets' clutching force. The commercial magnets of the prototypes can reliably work with up to three modules, but this number can be increased by using electromagnets with a higher clutching force (either larger or custom designs).

Stacking modules might be the most advantageous way to obtain a high number of states, but when space is limited, alternative ways to expand the reachable workspace of this class of mechanisms can be considered. The conceptual designs presented in the first part of this section have up to four different

states because of the classical configuration of kinematic couplings, which favors a triangular layout. However, alternative concepts with more than four states per module can be designed if needed. Since at least two pin/ball contacts are needed to pivot from a state to another, any design that aims at five or more states per platform leads to a kinematic coupling with redundant constraints in the neutral state, which will affect the positioning accuracy [32] and need to be carefully designed not to reduce performance.

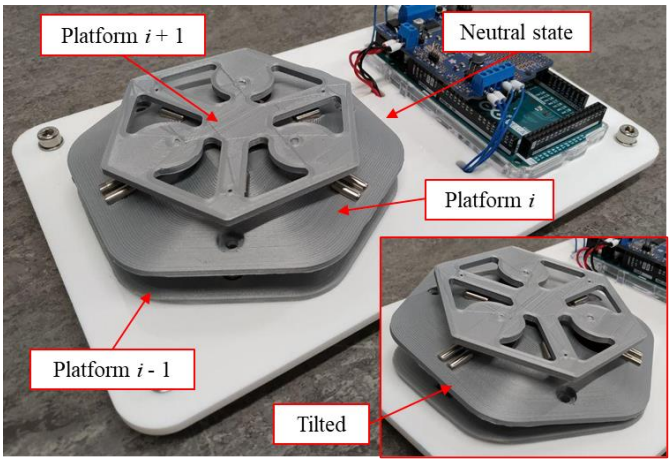

Fig. 8. A prototype of a modular 2D concept assembled with 3D-printed and laser-cut components, and with commercial electronics.

IV. Analysis of Designs with a Regular Layout

An analysis of the proposed binary mechatronic system is here presented. The kinematics of the proposed concept are illustrated and a procedure for the synthesis of a mechanism capable of reaching a given number of prescribed desired poses is discussed with two examples. The results in this section focus on platform designs that are based on regular polygons, whereas a study of irregular designs with asymmetric platform layouts and/or stacked architectures with variable module designs can be found in Section V.

A. Kinematic analysis of designs with a regular layout

A solution to the kinematic problem of the proposed binary mechatronic system is here reported with a focus on the example introduced in Section III-B, based on a Three-Groove kinematic coupling and a triangular layout with four states. However, the equations are written in a generic way that can be adapted to systems with more states when their layout is based on a regular polygon, with examples in Fig. 9a. The number of states of such systems can be easily calculated as 1 + s, where s is the number of sides of the regular polygon and the additional state is the neutral state. Thus, the Three-Groove concept is a particular case (s = 3) of a wider class of mechanisms.

In each state, the position of the top platform depends on the geometrical parameters of the design, which are summarized in Fig. 9. Each state is defined by a transformation matrix that describes the location of the central point H of the top platform, with respect to the central point O of the base. These two points coincide when the system is in the neutral state (0). Non-neutral states are described by a rotation of θ around an axis defined by the kinematic coupling features around which the top platform is pivoting, as previously shown in Table IV.

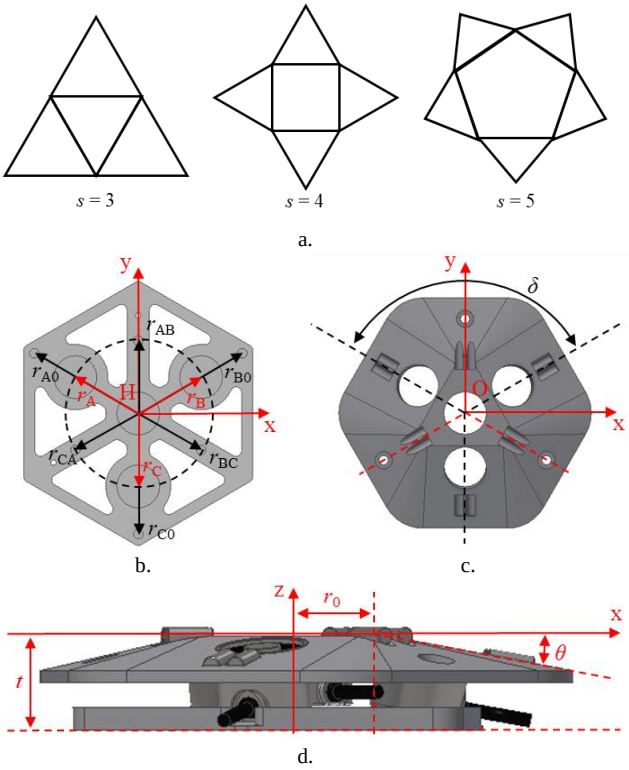

Fig. 9. Design parameters of the proposed concept: a. Examples of module layout based on regular polygons with s non-neutral states; b. Geometrical parameters of the top platform with position vectors of the main points; c. Orientation of the pins of the kinematic coupling on the base; d. Bending angle.

For any regular polygon with s sides, the rotation matrix of the i-th state can be written as

$$\boldsymbol{R_i}(\theta,\delta) = \mathbf{rot_z}(i\delta)\cdot\mathbf{rot_x}(\theta)\cdot\mathbf{rot_z}(-i\delta) \quad (1)$$

where θ and δ are geometrical parameters of the system, as shown in Fig. 9, and the latter can be computed as $\delta = 2\pi/s$. The position of point H in the i-th state can be computed as

$$\boldsymbol{p_i}(\theta,\delta,r_0) = \mathbf{rot_z}(i\delta)\cdot[0 \quad r_0(\cos\theta - 1) \quad r_0\sin\theta]^T \quad (2)$$

where r_0 is given by

$$r_0 = r_i\cos(\pi - \delta) \quad (3)$$

when evaluated for the proposed layout. Thus, the transformation matrix of the i-th state is defined as

$$\boldsymbol{T_i} = \begin{bmatrix} \boldsymbol{R_i} & \boldsymbol{p_i} \\ \mathbf{0}_{1\times3} & \mathbf{1}_{1\times1} \end{bmatrix} \text{ for } i = \{1, 2, \dots, s\} \quad (4)$$

B. Mechanism synthesis of designs with a regular layout

The fundamental problem behind the kinematic synthesis of mechanisms is to determine the design parameters to reach a given number of prescribed desired frames, as exemplified in Fig. 10. Given the finite number of states that a binary-actuated system can reach, the solution to the problem might look trivial, but as the number of desired frames increases, so does the complexity of the problem [17]. Furthermore, while a single optimization problem can provide solutions to the dimensional synthesis of a binary mechatronic system with a given architecture module, the computation of an optimal number of modules in series is a distinct problem that depends on the prescribed desired frames.

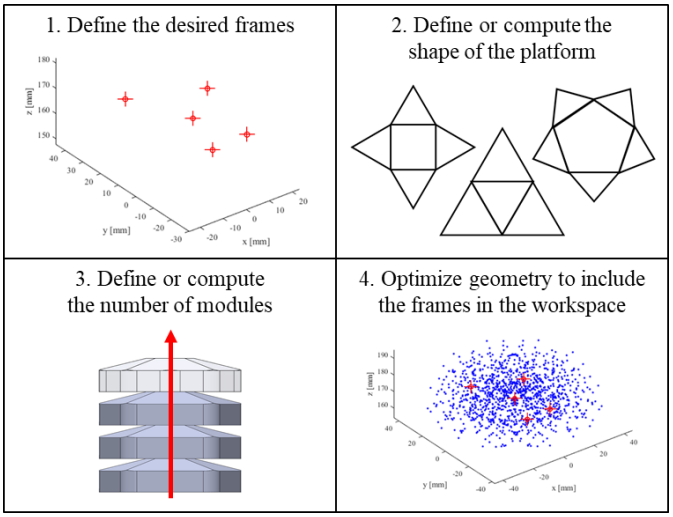

Fig. 10. Main steps of an algorithm for the synthesis of the proposed class of mechanisms. Given a certain number of points that must be reached with a given orientations, the algorithm finds the shape of the platform for each module, the number of modules in the system, and/or the geometrical parameters of each module in order to achieve all the desired poses.

1) Optimization Parameters

The following independent module parameters can be identified from the kinematic analysis: θ, s, and r_0. The thickness t of each module is also needed for the transformation from top platform to base of the following module, which is defined as a translation of t along the z-axis.

Furthermore, an additional parameter m can be used to describe the number of consecutive modules in the system. As discussed in Section III, the number of possible states of such a combined system is equal to n^m, where m is the number of modules and n is the number of states of each module, which is equal to $1 + s$. Thus, if m_F represents the number of desired frames, this condition can be expressed as

$$(1+s)^m \geq m_F \tag{5}$$

Therefore, given a module design with a known geometry, the number of modules can be computed as

$$m \geq \frac{\ln m_F}{\ln(1+s)} \tag{6}$$

where m, m_F, and s are all integers.

2) Kinematic Synthesis

The kinematic synthesis can be addressed in three ways:

- For a given number of modules, find module design parameters θ, s, r_0, t. This approach is the most efficient at constraining the search to a limited number of modules, which can be convenient, for example, is case of low clutch payload.
- For a given module geometry, find module number m. This approach is particularly useful to reconfigure existing modules to new tasks but should not be used for kinematic synthesis, as it can result in over-engineered systems with many unrequired modules.
- Optimize the full parameter set (θ, s, r_0, t, m). This approach solves a general optimization problem, with a long time to solution but the best results.

C. Examples of designs with a regular layout

To validate the proposed models, two examples of architectural and dimensional synthesis are here solved by using a genetic algorithm. The main challenge is the mixed nature of the set of parameters: θ, r_0, and t are positive real numbers, stored as double-precision floating-point values, whereas s and m are integer-valued variables. This limits the optimization methods to the ones able of mixed integer programming. In the following examples, a mixed integer genetic algorithm has been used to compute the optimal design for two positioning operations, with 5 and 20 prescribed poses. The problem was solved as a constrained minimization with the set of constraints shown in Table V and run in MATLAB R2020a on a Windows 10 computer with a 2.60 GHz quad-core CPU (Intel i7-6700HQ).

TABLE V
RESULTS OF EXAMPLES I AND II (REGULAR POLYGONS)

Parameter	Lower limit	Upper limit	Example i	Example ii
θ	π/24 rad	π/6 rad	0.28 rad	0.19 rad
s	3	6	5	5
r_0	10 mm	200 mm	28.7 mm	37.0 mm
t	25 mm	200 mm	38.6 mm	34.9 mm
m	1	5	4	5

The first example (i) was run for the five prescribed positions in Table VI, with the results shown in Fig. 11 and 12. The time to solution was 4 min 11 sec, with a residual error of 0.34 mm. A second example (ii) was run for the 20 randomly generated positions in Table VII, with the results shown in Fig. 11b and 13b. The time to solution was 37 min 53 sec, with a residual error of 0.57 mm. The resulting sets of parameters for the first (i) and second (ii) examples are reported in Table V.

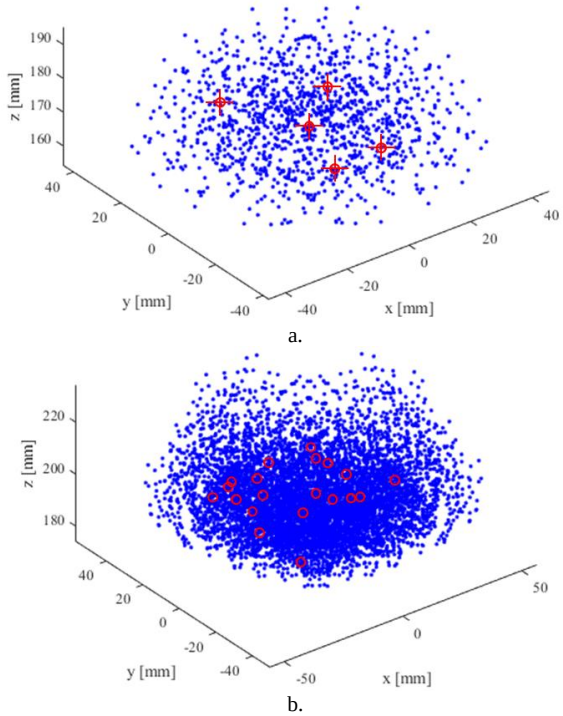

Fig. 11. Plot of the results of the kinematic synthesis: a. Reachable workspace for example i, with the target prescribed points shown in Table VI marked in red; b. Reachable workspace for example ii, with the target prescribed points shown in Table VIII marked in red.

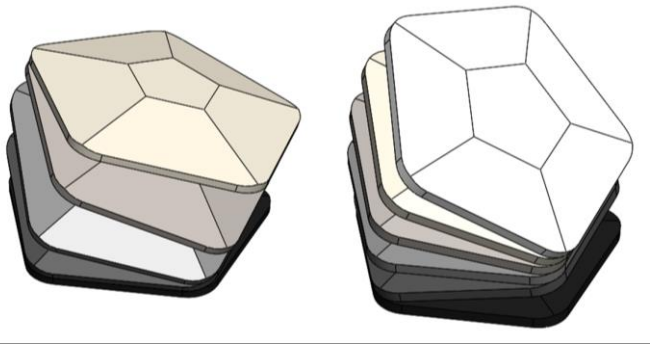

a. b.

Fig. 12. Results of the kinematic synthesis for regular designs: a. Geometrical model of the solution for example i, with 4 pentagonal modules and a tilt angle of 16°; b. A representation of the solution for example ii, with 5 pentagonal modules and a tilt angle of 11°.

TABLE VI
PRESCRIBED POINTS FOR EXAMPLES I, III, IV AND V

Frame	x [mm]	y [mm]	z [mm]
1	0.0	0.0	170.0
2	10.0	5.0	176.0
3	8.0	-20.0	170.0
4	-10.0	-24.0	172.0
5	25.0	10.0	180.0

TABLE VII
PRESCRIBED POINTS FOR EXAMPLE II

Frame	x [mm]	y [mm]	z [mm]	Frame	x [mm]	y [mm]	z [mm]
1	-22.0	18.0	201.0	11	-29.0	17.0	200.0
2	-19.0	8.0	195.0	12	27.0	-10.0	199.0
3	4.0	-6.0	198.0	13	-29.0	4.0	205.0
4	13.0	15.0	201.0	14	-11.0	13.0	196.0
5	-30.0	-10.0	199.0	15	3.0	28.0	197.0
6	21.0	9.0	195.0	16	-28.0	-30.0	196.0
7	20.0	27.0	197.0	17	7.0	-12.0	200.0
8	-15.0	25.0	197.0	18	-9.0	19.0	199.0
9	0.0	-2.0	200.0	19	11.0	6.0	204.0
10	10.0	-13.0	200.0	20	-12.0	-10.0	200.0
10	10.0	-13.0	200.0	20	-12.0	-10.0	200.0

By changing the optimization algorithm and constraints, this procedure can be adapted to any synthesis problem. When exact positioning is needed, however, the number of optimization parameters should be reduced, or alternative procedures should be considered. Once the optimal design for the proposed binary mechatronic system has been defined, sensorless control can be achieved. The main sources of error can be identified as the manufacturing and assembly tolerances, and as the dimensional tolerance of the kinematic synthesis (i.e. the residual error of the genetic algorithm optimization in the examples), which can be reduced by refining the algorithm. A calibration of the system compensates these errors by measuring the position and orientation of the manipulator in all the relevant states. Therefore, it is possible to assume that the mechanism will achieve a calibrated state every time with an error within the repeatability of the kinematic coupling, which can be as small as 20 μm and can be estimated as described in [32].

V. ANALYSIS OF IRREGULAR AND ASYMMETRIC DESIGNS

A. *Designs with an asymmetric module layout*

The kinematics presented in Section IV-A assume module geometry with axial symmetry, based on regular shapes. However, when the desired prescribed frames have an irregular distribution in the workspace, asymmetric designs based on non-regular polygons can be also considered to reduce the number of modules and/or actuators of the proposed mechatronic system, or to improve its performance.

When a general (non-regular) polygon with s sides is used, each state will be described by a given δ_i value, subject to

$$\sum_{i=1}^{s} \delta_i = 2\pi \quad (7)$$

Thus, the rotation matrix for the i-th state can be written as

$$\boldsymbol{R_i}(\theta, \delta_i) = \mathbf{rot_z}(\delta_i) \cdot \mathbf{rot_x}(\theta) \cdot \mathbf{rot_z}(-\delta_i), \quad (8)$$

and the position of point H in the i-th state can be computed as

$$\boldsymbol{p_i}(\theta, \delta_i, r_0) = \mathbf{rot_z}(\delta_i) \cdot [0 \quad r_0(\cos\theta - 1) \quad r_0 \sin\theta]^T \quad (9)$$

This asymmetry can also be included in other variables, such as θ and r_0, by assigning to those variables a value for each state.

Asymmetric module designs can be used to improve the results of the optimization procedure described in Section IV-B by introducing additional optimization parameters. As an example, the synthesis procedure for the points in Table VI is run again for an asymmetric design with variable δ and θ. The optimization parameters are shown in Table VIII with their minimum and maximum values. The optimization results were obtained after 6 min 47 sec of computation, with a residual error of 0.45 mm. The resulting set of parameters is listed in Table VIII (example iii), with the corresponding reachable workspace shown in Fig. 13. The final design is graphically represented in the diagram of Fig. 14a and the model in Fig. 14c.

When compared to the results obtained with a regular design on the same points (Table V, example i), the asymmetric design demonstrates its flexibility in terms of a reduced number of modules needed to achieve equivalent results, three rather than four. Furthermore, the asymmetric design enables a leaner architecture with less actuators per module, with four non-neutral states rather than five. In the given comparison, however, the residual of example iii is 25% higher than the residual of example i. For this reason, a further example of asymmetric module design synthesis is reported to show that, for a constant number of modules m, asymmetric designs can still perform better than regular layouts.

TABLE VIII
RESULTS OF EXAMPLES III AND IV (ASYMMETRIC DESIGNS)

Parameter	Lower limit	Upper limit	Example iii	Example iv
θ_1	π/24 rad	π/6 rad	0.22 rad	0.29 rad
θ_2	π/24 rad	π/6 rad	0.36 rad	0.15 rad
θ_3	π/24 rad	π/6 rad	0.52 rad	0.13 rad
θ_4	π/24 rad	π/6 rad	0.14 rad	0.47 rad
δ_1	π/6 rad	π rad	0.65 rad	0.72 rad
δ_2	π/6 rad	π rad	0.59 rad	1.31 rad
δ_3	π/6 rad	π rad	2.89 rad	1.16 rad
δ_4	π/6 rad	π rad	2.15 rad	3.09 rad
s	3	6	4	4
r_0	10 mm	200 mm	25.2 mm	27.4 mm
t	25 mm	200 mm	53.2 mm	40.6 mm
m	1	5	3	4

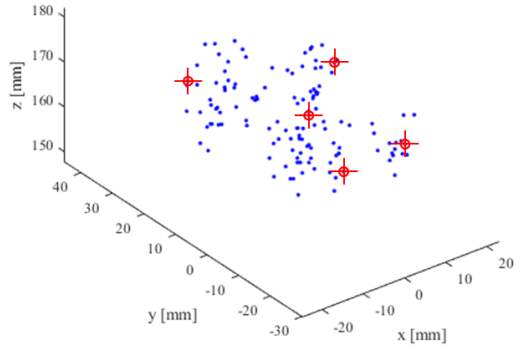

a.

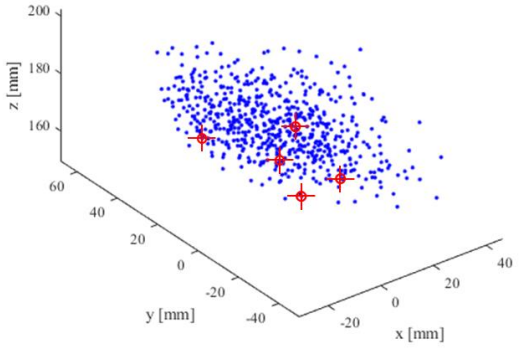

b.

Fig. 13. Plot of the results of the kinematic synthesis: a. Reachable workspace for example iii, with the target prescribed points shown in Table VI marked in red; b. Reachable workspace for example iv, with the target prescribed points shown in Table VI marked in red.

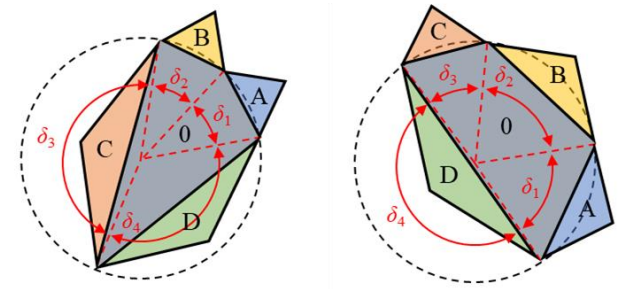

a. b.

c. d.

Fig. 14. Results of the kinematic synthesis for asymmetric designs: a. Schematic top view of the asymmetric platform design with the parameters in Table VIII and the five possible states (0, A, B, C, and D) for example iii; b. Schematic top view of the asymmetric platform design with the parameters in Table VIII and the five possible states (0, A, B, C, and D) for example iv; c. Geometrical model of the solution for example iii, with 3 quadrilateral modules and tilt angles of 13°/20°/30°/8°; d. A representation of the solution for example iv, with 4 quadrilateral modules and tilt angles of 17°/9°/7°/27°.

To obtain the results for example iv, the number of sections was not included in the set of optimization parameters, and a value of 4 was assigned to the *m* variable. The genetic algorithm optimization converged to a local minimum with a residual error of 0.23 mm, lower than the one of the previous examples on the same dataset (i and iii). However, the time to solution increased significantly because of the additional variables: the optimization results were obtained after 14 min 53 sec of computation. The resulting set of parameters is listed in Table VIII (example iv), with the corresponding reachable workspace shown in Fig. 13b. The final design is graphically represented in the diagram of Fig. 14b and the model in Fig. 14d.

Further tests were performed on randomly generated frames, and asymmetric designs have consistently resulted in less modules and actuators than designs based on regular polygons (iii). Moreover, asymmetric designs outperform regular layouts with the same number of modules on prescribed tasks (iv). In conclusion, an asymmetric module design is the optimal choice for a prescribed positioning operation, whereas a regular design fares better in scenarios that require higher flexibility. As irregular designs still work by translating between two kinematic coupling sharing four out of six contacts as seen in the 3D prototype, the experimental results obtained in Section II-B can be expanded to include these more general cases.

B. Irregular architectures with variable module design

In the previous examples, the combination of multiple modules to achieve a desired number of frames assumed the same module geometry throughout the system. However, modules with distinct designs can be stacked to further enlarge the design space. A variable module design implies 4*m* parameters, as each section is now defined by 4 independent variables (θ, s, r_0, and t).

A last example (v) of kinematic synthesis is here reported under the following assumptions: fixed number of modules with variable geometry (m = 4) and regular layout; constraints as per Table V; and desired frames as per Table VI. Thus, the only difference between the examples i and v is the assumption of same module geometry throughout the system in case i.

The time to solution of example v was 6 min 39 sec. As expected from the larger set of optimization parameters, the residual was 0.28 mm, better than example i. The resulting set of parameters is listed in Table IX, with significant differences between modules, including their shapes: one square module followed by three pentagonal ones, all with different geometries. The reachable workspace for example v is shown in Fig. 15a, whereas a graphical representation of the resulting mechatronic system can be found in Fig. 15b.

TABLE IX
RESULTS OF EXAMPLE V (VARIABLE MODULE DESIGN)

Parameter	Module 1	Module 2	Module 3	Module 4
θ	0.28 rad	0.32 rad	0.31 rad	0.33 rad
s	4	5	5	5
r_0	58.7 mm	51.6 mm	33.0 mm	18.4 mm
t	35.7 mm	34.4 mm	30.4 mm	43.6 mm

In order to further improve the performance of the proposed class of mechanisms, architectures with variable, asymmetric module designs can be designed by adopting the procedures described in both Section V-A and Section V-B. However, the exponential kinematic behavior of binary-actuated mechanisms

can result in prohibitive computation times. Furthermore, highly asymmetric and irregular mechanisms can be challenging to design and manufacture. Thus, it is advisable to find a balance between complexity and performance.

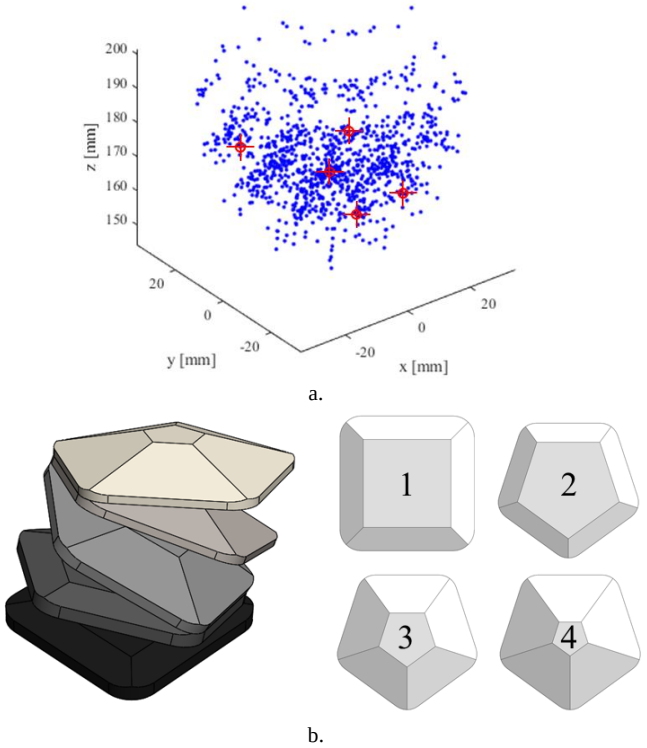

Fig. 15. Results of the kinematic synthesis for irregular designs: a. Reachable workspace for example v, with the prescribed points shown in Table VI in red; b. A representation of the solution for example v, with a quadrilateral module with a tilt angle of 16° and 3 pentagonal modules with tilt angles of 18°/18°/19°.

VI. Conclusion

High-precision positioning mechanisms are required in many fields, from manufacturing to space exploration and biomedical applications. In the last decades, mechatronic devices with binary actuators have been identified as a potential solution, thanks to their simple and robust design. Furthermore, their reliance on mechanical stops for positioning provides high repeatability. In this paper, a novel class of binary-actuated mechanisms based on kinematic couplings and driven by electromagnets was introduced. The proposed concept is characterized with a kinematic model, and a synthesis procedure is discussed for the task-oriented design of this class of binary-actuated manipulators. Further results of this work are summarized in the following points:

- *Experimental validation:* Two prototypes were presented to validate the concept and to demonstrate its modularity. The prototypes are comparable in size to previous discrete mechanisms, but could be further scaled down by using custom electromagnets rather than commercial ones.
- *Kinematic analysis:* The kinematic behavior of the proposed class of manipulators was modeled.
- *Methods for kinematic synthesis:* Three procedures for the kinematic synthesis of the proposed class of manipulators were discussed. Given the desired prescribed frames to reach, a first procedure, from literature, computed the design of a module; the second one evaluated the number of modules to stack to achieve the target frames; the third one optimized all the parameters with a genetic algorithm.
- *Mixed-integer optimization for kinematic synthesis:* The proposed method requires the optimization of both integer and real numbers, and conventional algorithms cannot handle this class of problems. Therefore, a formulation for a mixed-integer optimization problem was reported and validated with simulations of randomly generated tasks.
- *Asymmetric and irregular designs:* The effect of asymmetries and irregularities in the proposed class of mechanisms was studied. Three examples were reported to identify the characteristics of these architectures.

The main advantages of the novel design over existing ones are summarized in the following points:

- *High precision:* Previous designs rely on the extreme positions of their binary actuators for reliability. The proposed design allows the manipulator to achieve accuracy and repeatability as good as manufacturing precision by using a kinematic coupling.
- *Sensorless control:* The system is in a stable state only if its two platforms are engaged through a kinematic coupling, according to the polarity of all the actuators. Thus, feedback is not required, simplifying both control and mechanical design, and reducing the overall cost.
- *Efficient transition between states:* The proposed device is controlled by electromagnets and transition is triggered by a switch in polarity. The transition is characterized by a low friction sliding motion of steel balls on steel pins.
- *Stability:* Some discrete actuators are sensitive to external disturbance, and their state can be changed by unexpected events. Since each state of the proposed system is maintained by an electromagnetic clutch, external loads lower than the clutching force do not affect the mechanism.

Overall, the novel class of mechanisms introduced in this paper is uniquely suited to a wide range of applications that require a rapid, accurate, and interchangeable positioning of sensors and tools.

References

[1] G. S. Chirikjian. “A binary paradigm for robotic manipulators.” In *Proc. IEEE Int. Conf. on Robotics and Automation*, pp. 3063-3069. IEEE, 1994.

[2] G. S. Chirikjian. “Kinematic synthesis of mechanisms and robotic manipulators with binary actuators.” *ASME Journal of Mechanical Design*, vol. 117, no. 4, pp. 573-580. 1995.

[3] I. Ebert-uphoff and G. S. Chirikjian. “Efficient workspace generation for binary manipulators with many actuators.” *Journal of Robotic Systems* vol. 12, no. 6, pp. 383-400. 1995.

[4] D. S. Lees and G. S. Chirikjian. “A combinatorial approach to trajectory planning for binary manipulators.” In *Proc. IEEE Int. Conf. on Robotics and Automation*, vol. 3, pp. 2749-2754. IEEE, 1996.

[5] D. S. Lees and G. S. Chirikjian. “An efficient method for computing the forward kinematics of binary manipulators.” In *Proc. IEEE Int. Conf. on Robotics and Automation*, vol. 2, pp. 1012-1017. IEEE, 1996.

[6] J. Suthakorn and G. S. Chirikjian. “A new inverse kinematics algorithm for binary manipulators with many actuators.” *Advanced Robotics* vol. 15, no. 2, pp. 225-244. 2001

[7] D. Schütz, A. Raatz and J. Hesselbach. “The development of a reconfigurable parallel robot with binary actuators.” In *Advances in Robot*

Kinematics: Motion in Man and Machine, pp. 225-232. Springer, Dordrecht, 2010.
[8] A. Motahari, H. Zohoor and M. Habibnejad Korayem. "Discrete kinematic synthesis of discretely actuated hyper-redundant manipulators." *Robotica* vol. 31, no. 7, pp. 1073-1084. 2013.
[9] A. Wingert, M. D. Lichter, S. Dubowsky and M. Hafez. "Hyper-redundant robot manipulators actuated by optimized binary-dielectric polymers." In *Smart Structures and Materials 2002: Electroactive Polymer Actuators and Devices (EAPAD)*, vol. 4695, pp. 415-423. International Society for Optics and Photonics, 2002.
[10] A. Wingert, M. D. Lichter and S. Dubowsky. "On the design of large degree-of-freedom digital mechatronic devices based on bistable dielectric elastomer actuators." *IEEE/ASME transactions on mechatronics* vol. 11, no. 4, pp. 448-456. 2006.
[11] J. S. Plante, L. M. Devita and S. Dubowsky. "A road to practical dielectric elastomer actuators based robotics and mechatronics: discrete actuation." In *Electroactive Polymer Actuators and Devices (EAPAD) 2007*, vol. 6524, p. 652406. International Society for Optics and Photonics, 2007.
[12] M. Hafez, M. D. Lichter and S. Dubowsky. "Optimized binary modular reconfigurable robotic devices." *IEEE/ASME transactions on mechatronics* vol. 8, no. 1, pp. 18-25. 2003
[13] V. A. Sujan and S. Dubowsky. "Design of a lightweight hyper-redundant deployable binary manipulator." *J. Mech. Des.* vol. 126, no.1, pp. 29-39. 2004.
[14] S. H. Jeong, K. R. Cha, H. U. Kim, S. B. Choi, G. H. Kim and J. H. Park. "A Study on the Mechanism of the Robot Hand based on the Segment Binary Control." In *Proceedings of the Korean Society of Precision Engineering Conference*, pp. 1232-1235. Korean Society for Precision Engineering, 2005.
[15] S. H. Jeong, J. H. Park, K. R. Cha, S. H. Ryu and G. H. Kim. "A study on driving mechanism of robot hand driven by SMA based on segmented binary control." *Transactions of the Korean Society of Machine Tool Engineers* vol. 15, no. 5, pp. 14-20. 2006.
[16] E. Tzorakoleftherakis, A. Mavrommati and A. Tzes. "Design and implementation of a binary redundant manipulator with cascaded modules." *Journal of Mechanisms and Robotics* vol. 8, no. 1. 2016.
[17] M. Keizo and G. S. Chirikjian. "General kinematic synthesis method for a discretely actuated robotic manipulator (D-ARM)." In *2006 IEEE/RSJ International Conference on Intelligent Robots and Systems*, pp. 5889-5894. IEEE, 2006.
[18] S. A. Zirbel, K. A. Tolman, B. P. Trease and L. L. Howell. "Bistable mechanisms for space applications." *PloS one* vol. 11, no. 12. 2016.
[19] T. Kamf and J. Abrahamsson. "Self-sensing electromagnets for robotic tooling systems: Combining sensor and actuator." *Machines* vol. 4, no. 3, pp. 16. 2016.
[20] Z. Zhang, D. Chen, H. Wu, Y. Bao and G. Chai. "Non-contact magnetic driving bioinspired Venus flytrap robot based on bistable anti-symmetric CFRP structure." *Composite Structures* vol. 135, pp. 17-22. 2016.
[21] Z. Zhang, X. Li, X. Yu, H. Chai, Y. Li, H. Wu and S. Jiang. "Magnetic actuation bionic robotic gripper with bistable morphing structure." *Composite Structures* vol. 229, pp. 111422. 2019.
[22] M. M. Kaluarachchi, J. H. Ho, S. Yahya and S. H. Teh. "Design of a bistable electromagnetic coupling mechanism for underactuated manipulators." *Smart Materials and Structures* vol. 27, no. 7, pp. 075031. 2018.
[23] S. Duque Tisnes, L. Petit, C. Prelle, and F. Lamarque. "Modeling and experimental validation of a planar micro conveyor based on a 2 x 2 array of digital electromagnetic actuators." *IEEE/ASME Transactions on Mechatronics*, 2020.
[24] W. Ma, Z. Zhang, H. Zhang, Y. Li, H. Wu, S. Jiang and G. Chai. "An origami-inspired cube pipe structure with bistable anti-symmetric CFRP shells driven by magnetic field." *Smart Materials and Structures* vol. 28, no. 2, pp. 025028. 2019.
[25] S. Gao, H. Zhou, P. Hu, J. Chen, J. Yang and N. Li. "A general framework of workpiece setup optimization for the five-axis machining." *Int. Journal of Machine Tools and Manufacture* 149 (2020): 103508.
[26] F. Ding, X. Luo, W. Zhong and W. Chang. "Design of a new fast tool positioning system and systematic study on its positioning stability." *Int. Journal of Machine Tools and Manufacture* 142 (2019): 54-65.
[27] C. H.,Schouten, P. C. J. N. Rosielle and P. H. J. Schellekens. "Design of a kinematic coupling for precision applications." *Precision Engineering* vol. 20 no. 1, pp. 46-52. 1997.
[28] L. C. Hale and A. H. Slocum. "Optimal design techniques for kinematic couplings." *Precision Engineering* vol. 25, no. 2, pp. 114-127. 2001.
[29] A. J. Hart, A. Slocum and P. Willoughby. "Kinematic coupling interchangeability." *Precision Engineering* vol. 28, no. 1, pp. 1-15. 2004.
[30] M. L. Culpepper. "Design of quasi-kinematic couplings." *Precision Engineering* vol. 28, no. 3, pp. 338-357. 2004.
[31] M. L. Culpepper, A. H. Slocum, F. Z. Shaikh and G. Vrsek. "Quasi-kinematic couplings for low-cost precision alignment of high-volume assemblies." *J. Mech. Des.* vol. 126, no. 3, pp. 456-463. 2004.
[32] A. Slocum. "Kinematic couplings: A review of design principles and applications." *Int. journal of machine tools and manufacture* vol. 50, no. 4, pp. 310-327. 2010.
[33] "Arduino Mega 2560 rev3." Arduino. [Online] Available: https://store.arduino.cc/arduino-mega-2560-rev3, Accessed on: Jun. 12, 2020.
[34] "Adafruit Motorshield v2." Adafruit. [Online] Available: https://www.adafruit.com/product/1438, Accessed on: Jun. 12, 2020.
[35] "5V Electromagnet - 2.5 Kg Holding Force - P20/15." Adafruit. [Online] Available: https://www.adafruit.com/product/3872, Accessed on: Jun. 12, 2020.
[36] "Eclipse Neodymium Magnet 0.9kg, Width 15mm". Eclipse. [Online] Available: https://docs.rs-online.com/127e/0900766b814a35c5.pdf, Accessed on: Jun. 12, 2020.

Matteo Russo (M'18) received the B.Sc., M.Sc. and Ph.D. degrees in mechanical engineering from the University of Cassino, Italy, in 2013, 2015, and 2019, respectively. Between 2015 and 2017 he was a visiting researcher at RWTH Aachen University, University of the Basque Country and Tokyo Institute of Technology.

Since 2019, he is a Research Fellow at the Rolls-Royce UTC in Manufacturing and On-Wing Technology, University of Nottingham, Nottingham, UK. His main research interests are continuum robots, robot kinematics and parallel manipulators.

Jorge Barrientos-Diez (M'19) received his B.Eng. degree in industrial electronics and automation engineering from the Technical University of Madrid in 2014 and his M.Sc. degree in industrial engineering from the same institution in 2017 with a year-long stay at INSA Lyon.

He is currently pursuing the Ph.D. degree at the University of Nottingham, Nottingham, UK, where he specialises in the design and control of small continuum robots. His research interests are in the design and control of novel robotic systems.

Dragos Axinte received the M.Eng. degree in manufacturing engineering in 1988, and the Ph.D. degree in manufacturing engineering in 1996.

After graduating, he worked in R&D in industry for 10 years and then moved to academia to lead research in the field of machining, process monitoring and design of innovative tooling/robotics for in-situ repair especially related to on-wing repair of aeroengines.

Currently, he is Professor of Manufacturing Engineering at University of Nottingham and Director of Rolls-Royce University Technology Centre (UTC) in Manufacturing and On-Wing Technology.